

## A Family of 3d-4f Octa-Nuclear $[\text{Mn}^{\text{III}}_4\text{Ln}^{\text{III}}_4]$ Wheels (Ln = Sm, Gd, Tb, Dy, Ho, Er, and Y): Synthesis, Structure, and Magnetism

Mengyuan Li,<sup>†,‡</sup> Yanhua Lan,<sup>†</sup> Ayuk M. Ako,<sup>†,§</sup> Wolfgang Wernsdorfer,<sup>||</sup> Christopher E. Anson,<sup>†</sup> Gernot Buth,<sup>⊥</sup> Annie K. Powell,<sup>\*,†,§</sup> Zheming Wang,<sup>\*,‡</sup> and Song Gao<sup>\*,‡</sup>

<sup>†</sup>Institut für Anorganische Chemie der Universität Karlsruhe, Karlsruhe Institute of Technology, Engesserstrasse 15, D-76131 Karlsruhe, Germany, <sup>‡</sup>Beijing National Laboratory for Molecular Sciences, State Key Laboratory of Rare Earth Materials Chemistry and Applications, College of Chemistry and Molecular Engineering, Peking University, Beijing 100871, China, <sup>§</sup>Institute for Nanotechnology, Forschungszentrum Karlsruhe, Karlsruhe Institute of Technology, Postfach 3640, D-76021 Karlsruhe, Germany, <sup>||</sup>Institut Néel CNRS, BP 166, 25 av. des Martyrs, F-38042 Grenoble, France, and <sup>⊥</sup>Institut für Synchrotron Strahlung (ISS), FZK, Karlsruhe Institute of Technology, Postfach 3640, D-76021 Karlsruhe, Germany

Received August 31, 2010

We present the syntheses, crystal structures, and magnetochemical characterizations for a family of isostructural  $[\text{Mn}_4\text{Ln}_4]$  compounds (Ln = Sm, Gd, Tb, Dy, Ho, Er, and Y). They were prepared from the reactions of formic acid, propionic acid, *N*-*n*-butyl-diethanolamine, manganese perchlorate, and lanthanide nitrates under the addition of triethylamine in MeOH. The compounds possess an intriguing hetero-octanuclear wheel structure with four  $\text{Mn}^{\text{III}}$  and four  $\text{Ln}^{\text{III}}$  ions alternatively arranged in a saddle-like ring, where formate ions act as key carboxylate bridges. In the lattice, the molecules stack into columns in a quasi-hexagonal arrangement. Direct current (dc) magnetic susceptibility measurements indicated the depopulation of the Stark components at low temperature and/or very weak antiferromagnetic interactions between magnetic centers. The zero-field alternating current (ac) susceptibility studies revealed that the compounds containing Sm, Tb, and Dy showed frequency-dependent out-of-phase signals, indicating they are single-molecule magnets (SMMs). Magnetization versus applied dc field sweeps on a single crystal of the Dy compound down to 40 mK exhibited hysteresis depending on temperatures and field sweeping rates, further confirming that the Dy compound is a SMM. The magnetization dynamics of the Sm and Y compounds investigated under dc fields revealed that the relaxation of the Sm compound is considered to be dominated by the two-phonon (Orbach) process while the Y compound displays a multiple relaxation process.

### Introduction

Single-molecule magnets (SMMs), the individual molecules that behave as magnets below a certain blocking

temperature,<sup>1</sup> have been the subject of deep studies and continuous development owing to their unique magnetic properties and potential applications in information storage or quantum computing.<sup>2</sup> To date, the search for SMMs was based primarily on the use of 3d metal ions.<sup>3–5</sup> Recently, the

\*To whom correspondence should be addressed. Fax: +49 721 608 8142 (A.K.P.), 86-10-62751708 (Z.W., S.G.). E-mail: powell@aoc.uni-karlsruhe.de (A.K.P.), zmw@pku.edu.cn (Z.W.), gaosong@pku.edu.cn (S.G.).

(1) (a) Wernsdorfer, W.; Sessoli, R. *Science* **1999**, *284*, 133. (b) Gatteschi, D.; Sessoli, R. *Angew. Chem., Int. Ed.* **2003**, *42*, 268. (c) Powell, A. K. *Nat. Chem.* **2010**, *2*, 351. (d) Bagai, R.; Christou, G. *Chem. Soc. Rev.* **2009**, *38*, 1011.

(2) (a) Leuenberger, M. N.; Loss, D. *Nature* **2001**, *410*, 789. (b) Bogani, L.; Wernsdorfer, W. *Nat. Mater.* **2008**, *7*, 179. (c) Henderson, J. J.; Koo, C.; Feng, P. L.; del Barco, E.; Hill, S.; Tupitsyn, I. S.; Stamp, P. C. E.; Hendrickson, D. N. *Phys. Rev. Lett.* **2009**, *103*, 017202.

(3) (a) Stamatatos, T. C.; Abboud, K. A.; Wernsdorfer, W.; Christou, G. *Angew. Chem., Int. Ed.* **2008**, *47*, 6694. (b) Stamatatos, T. C.; Abboud, K. A.; Wernsdorfer, W.; Christou, G. *Angew. Chem., Int. Ed.* **2006**, *45*, 4134. (c) Yang, E. C.; Wernsdorfer, W.; Zakharov, L. N.; Karaki, Y.; Yamaguchi, A.; Isidro, R. M.; Lu, G. D.; Wilson, S. A.; Rheingold, A. L.; Ishimoto, H.; Hendrickson, D. N. *Inorg. Chem.* **2006**, *45*, 529. (d) Oshio, H.; Nihei, M.; Koizumi, S.; Shiga, T.; Nojiri, H.; Nakano, M.; Shirakawa, N.; Akatsu, M. *J. Am. Chem. Soc.* **2005**, *127*, 4568. (e) Hoshino, N.; Ako, A. M.; Powell, A. K.; Oshio, H. *Inorg. Chem.* **2009**, *48*, 3396, and references therein. (f) Lecren, L.; Roubeau, O.; Coulon, C.; Li, Y. G.; Le Goff, X. F.; Wernsdorfer, W.; Miyasaka, H.; Clérac, R. *J. Am. Chem. Soc.* **2005**, *127*, 17353.

(4) (a) Zheng, Y.-Z.; Tong, M.-L.; Zhang, W.-X.; Chen, X.-M. *Angew. Chem., Int. Ed.* **2006**, *45*, 6310. (b) Zeng, M. H.; Yao, M. X.; Liang, H.; Zhang, W. X.; Chen, X. M. *Angew. Chem., Int. Ed.* **2007**, *46*, 1832. (c) Zhang, Y. Z.; Wernsdorfer, W.; Pan, F.; Wang, Z. M.; Gao, S. *Chem. Commun.* **2006**, 3302. (d) Tasiopoulos, A. J.; Vinslava, A.; Wernsdorfer, W.; Abboud, K. A.; Christou, G. *Angew. Chem., Int. Ed.* **2004**, *43*, 2117. (e) Stamatatos, T. C.; Nastopoulos, V.; Tasiopoulos, A. J.; Moushi, E. E.; Wernsdorfer, W.; Christou, G.; Perlepes, S. P. *Inorg. Chem.* **2008**, *47*, 10081. (f) Saalfrank, R. W.; Scheurer, A.; Bernt, I.; Heinemann, F. W.; Postnikov, A. V.; Schunemann, V.; Trautwein, A. X.; Alam, M. S.; Rupp, H.; Müller, P. *Dalton Trans.* **2006**, 2865.

(5) (a) Milios, C. J.; Inglis, R.; Vinslava, A.; Bagai, R.; Wernsdorfer, W.; Parsons, S.; Perlepes, S. P.; Christou, G.; Brechin, E. K. *J. Am. Chem. Soc.* **2007**, *129*, 12505. (b) Milios, C. J.; Vinslava, A.; Wernsdorfer, W.; Moggach, S.; Parsons, S.; Perlepes, S. P.; Christou, G.; Brechin, E. K. *J. Am. Chem. Soc.* **2007**, *129*, 2754. (c) Accorsi, S.; Barra, A. L.; Caneschi, A.; Chastanet, G.; Cornia, A.; Fabretti, A. C.; Gatteschi, D.; Mortalo, C.; Olivieri, E.; Parenti, F.; Rosa, P.; Sessoli, R.; Sorace, L.; Wernsdorfer, W.; Zoppi, L. *J. Am. Chem. Soc.* **2006**, *128*, 4742. (d) Foguet-Albiol, D.; Abboud, K. A.; Christou, G. *Chem. Commun.* **2005**, 4282.

design and synthesis of heterometallic 3d-4f clusters have caught great attention since the discovery that such complexes are potential SMMs.<sup>6</sup> Lanthanide (Ln) metal ions bring a large ground-state spin and, in some cases, a strong easy axis anisotropic magnetic moment.<sup>7</sup> Therefore, the incorporation of Ln ions into such molecules has been recognized as an appealing route to new SMMs.<sup>6,8</sup> Recent years have witnessed an explosion in the research devoted to 3d-4f clusters,<sup>6,8-10</sup> with a particular emphasis on Mn-Ln based SMMs.<sup>9,10</sup> Mn<sup>III</sup> ion, with its uniaxial anisotropy, is the most widely known metal ion for constructing SMMs. Since the first discovery of the SMM, [Mn<sub>12</sub>OAc],<sup>1a</sup> complexes with nuclearity as high as [Mn<sub>84</sub>] have been reported.<sup>11</sup> To date, a few reports of heterometallic Mn-Ln systems have been documented such as [Mn<sub>7</sub>Ln<sub>2</sub>],<sup>10d</sup> [Mn<sub>6</sub>Dy<sub>6</sub>],<sup>9d</sup> [Mn<sub>11</sub>Dy<sub>4</sub>],<sup>9f</sup> [Mn<sub>11</sub>Gd<sub>2</sub>],<sup>10f</sup> [Mn<sub>5</sub>Ln<sub>4</sub>],<sup>10b</sup> [Mn<sub>10</sub>Ln<sub>2</sub>]<sup>10c</sup> (Ln = Pr and Nd), and so forth, but most of them lack systematic magnetic studies on a family of isostructural aggregates in which the 4f ion is varied across the series. Such systematic investigation may help to explore the correlation of magnetic properties with structural parameters and how the interplay of the mixed 3d and 4f ions can be optimized to produce SMMs.<sup>10d,e</sup> Therefore, further examples of high nuclearity Mn-Ln series compounds are expected.

One of the factors that prevent scientists from constructing 3d-4f SMMs is the synthetic difficulty considering the low stereochemical preferences of 4f ions. Diethanolamine ligands

and related polyodal ligands containing an N-donor function are widely employed for the assembly of polynuclear 3d species;<sup>12</sup> there are limited examples of 3d-4f clusters derived from this class of ligands.<sup>10b,d,f</sup> In fact, such ligands are suitable for coordinating 3d-4f metal ions because the chemical characteristics of the polydentate (N and O) can fulfill the coordinating affinities of 3d and 4f metal ions for N and O atoms. Ancillary ligands, such as carboxylate, are employed as bridging ligands or to meet the coordination spheres of metal ions. Formate ion, the smallest and simplest carboxylate, possesses all the functionalities of carboxylate. Its small stereo effect is beneficial for the formation of extended structures, and it can adopt various bridging modes such as *syn-syn*, *anti-anti*, *syn-syn/anti* and provide significant magnetic coupling between spin carriers, leading to the occurrence of interesting and complicated magnetic systems.<sup>13-16</sup> However, the role of formate ion in constructing polynuclear metal clusters is less explored, though its use in search for new 3d-transition magnetic clusters has been recognized.<sup>17</sup> The incorporation of formate ion as key carboxylate into such system to produce heteropolynuclear 3d-4f complexes with SMM behavior has not been investigated.

Very recently, we have reported two heteropolynuclear 3d-4f wheel complexes Mn<sub>4</sub>Ln<sub>4</sub> (Ln = Gd and Dy), and the wheel containing anisotropic Dy<sup>III</sup> ions shows SMM behavior.<sup>18</sup> Indeed, several wheel-shaped SMMs have been reported, mainly composed of transition metal (TM) ions, such as [Mn<sub>n</sub>] (n = 16, 22, 24, 84), [Co<sub>8</sub>], [Fe<sub>9</sub>], and [Ni<sub>12</sub>], and so forth.<sup>19</sup> Heterometallic 3d-4f wheel-shaped SMMs are still rare.<sup>20</sup> As a continuation of our preliminary study, we present here the first family of Mn<sup>III</sup>-Ln<sup>III</sup> heterometallic octanuclear [Mn<sub>4</sub>Ln<sub>4</sub>] ring compounds with the formula of [Mn<sup>III</sup><sub>4</sub>Ln<sup>III</sup><sub>4</sub>(<sup>n</sup>Bu-dea)<sub>4</sub>(μ<sub>3</sub>-HCOO)<sub>4</sub>(μ-OMe)<sub>4</sub>(μ-O<sub>2</sub>CET)<sub>4</sub>(O<sub>2</sub>CET)<sub>4</sub>(MeOH)<sub>4</sub>] for

(6) (a) Andruh, M.; Costes, J. P.; Diaz, C.; Gao, S. *Inorg. Chem.* **2009**, *48*, 3342. (b) Sessoli, R.; Powell, A. K. *Coord. Chem. Rev.* **2009**, *253*, 2328. (c) Shiga, T.; Onuki, T.; Matsumoto, T.; Nojiri, H.; Newton, G. N.; Hoshino, N.; Oshio, H. *Chem. Commun.* **2009**, 3568.

(7) Kahn, O. *Molecular Magnetism*; VCH: New York, 1993.

(8) (a) Ako, A. M.; Mereacre, V.; Clérac, R.; Hewitt, I. J.; Lan, Y.; Buth, G.; Anson, C. E.; Powell, A. K. *Inorg. Chem.* **2009**, *48*, 6713. (b) Akhtar, M. N.; Mereacre, V.; Novitchi, Gh.; Tucheague, J.-P.; Anson, C. E.; Powell, A. K. *Chem.—Eur. J.* **2009**, *15*, 7278. (c) Mereacre, V. M.; Ako, A. M.; Clérac, R.; Wernsdorfer, W.; Filoti, G.; Bartolomé, J.; Anson, C. E.; Powell, A. K. *J. Am. Chem. Soc.* **2007**, *129*, 9248.

(9) (a) Zhang, M.-B.; Zhang, J.; Zheng, S.-T.; Yang, G.-Y. *Angew. Chem., Int. Ed.* **2005**, *44*, 1385. (b) Kong, X.-J.; Ren, Y.-P.; Long, L.-S.; Zheng, Z.; Huang, R.-B.; Zheng, L.-S. *J. Am. Chem. Soc.* **2007**, *129*, 7016. (c) Xu, G. F.; Wang, Q. L.; Gamez, P.; Ma, Y.; Clérac, R.; Tang, J. K.; Yan, S. P.; Cheng, P.; Liao, D. Z. *Chem. Commun.* **2010**, 1506. (d) Zaleski, C. M.; Depperman, E. C.; Kampf, J. W.; Kirk, M. L.; Pecoraro, V. L. *Angew. Chem., Int. Ed.* **2004**, *43*, 3912. (e) Okazawa, A.; Nogami, T.; Nojiri, H.; Ishida, T. *Inorg. Chem.* **2008**, *47*, 9763. (f) Mishra, A.; Wernsdorfer, W.; Abboud, K. A.; Christou, G. *J. Am. Chem. Soc.* **2004**, *126*, 15648. (g) Osa, S.; Kido, T.; Matsumoto, N.; Re, N.; Pochaba, A.; Mrozinski, J. *J. Am. Chem. Soc.* **2004**, *126*, 420. (h) Shiga, T.; Onuki, T.; Matsumoto, T.; Nojiri, H.; Newton, G. N.; Hoshino, N.; Oshio, H. *Chem. Commun.* **2009**, 3568.

(10) (a) Brechin, E. K. *Chem. Commun.* **2005**, 5141. (b) Mereacre, V.; Ako, A. M.; Clerac, R.; Wernsdorfer, W.; Hewitt, I. J.; Anson, C. E.; Powell, A. K. *Chem.—Eur. J.* **2008**, *14*, 3577. (c) Mereacre, V.; Prodius, D.; Ako, A. M.; Kaur, N.; Lipkowsky, J.; Simmons, C.; Dalal, N.; Geru, I.; Anson, C. E.; Powell, A. K.; Turta, C. *Polyhedron* **2008**, *27*, 2459. (d) Mereacre, V.; Lan, Y. H.; Clerac, R.; Ako, A. M.; Hewitt, I. J.; Wernsdorfer, W.; Buth, G.; Anson, C. E.; Rowell, A. K. *Inorg. Chem.* **2010**, *49*, 5293. (e) Ako, A. M.; Mereacre, V.; Clerac, R.; Hewitt, I. J.; Lan, Y. H.; Buth, G.; Anson, C. E.; Powell, A. K. *Inorg. Chem.* **2009**, *48*, 6713. (f) Mereacre, V. M.; Ako, A. M.; Clérac, R.; Wernsdorfer, W.; Filoti, G.; Bartolomé, J.; Anson, C. E.; Powell, A. K. *J. Am. Chem. Soc.* **2007**, *129*, 9248.

(11) (a) Murugesu, M.; Raftery, J.; Wernsdorfer, W.; Christou, G.; Brechin, E. K. *Inorg. Chem.* **2004**, *43*, 4203. (b) Manoli, M.; Prescimone, A.; Mishra, A.; Parsons, S.; Christou, G.; Brechin, E. K. *Dalton Trans.* **2007**, 532. (c) Tasiopoulos, A. J.; Vinslava, A.; Wernsdorfer, W.; Abboud, K. A.; Christou, G. *Angew. Chem., Int. Ed.* **2004**, *43*, 2117.

(12) (a) Murugesu, M.; Habrych, M.; Wernsdorfer, W.; Abboud, K. A.; Christou, G. *J. Am. Chem. Soc.* **2004**, *126*, 4766. (b) Shah, S. J.; Ramsey, C. M.; Heroux, K. J.; O'Brien, J. R.; DiPasquale, A. G.; Rheingold, A. L.; del Barco, E.; Hendrickson, D. N. *Inorg. Chem.* **2008**, *47*, 6245. (c) Saalfrank, R. W.; Scheurer, A.; Prakash, R.; Heinemann, F. W.; Nakajima, T.; Hampel, F.; Leppin, R.; Pilawa, B.; Rupp, H.; Müller, P. *Inorg. Chem.* **2007**, *46*, 1586. (d) Saalfrank, R. W.; Prakash, R.; Maid, H.; Hampel, F.; Heinemann, F. W.; Trautwein, A. X.; Böttger, L. H. *Chem.—Eur. J.* **2006**, *12*, 2428.

(13) (a) Sun, Q.; Yue, Q.; Zhang, J. Y.; Wang, L.; Li, X.; Gao, E. Q. *Cryst. Growth Des.* **2009**, *9*, 2310. (b) Colacio, E.; Ghaze, M.; Kivekäs, R.; Moreno, J. M. *Inorg. Chem.* **2000**, *39*, 2882. (c) Poulsen, R. D.; Jorgensen, M. R. V.; Overgaard, J.; Larsen, F. K.; Morgenroth, W. G.; Graber, T.; Chen, Y. S.; Iversen, B. B. *Chem.—Eur. J.* **2007**, *13*, 9775, and references therein.

(14) (a) Zhang, X. F.; Hu, T. L.; Bu, X. H. *Dalton Trans.* **2008**, 56. (b) Zhao, J. P.; Hu, B. W.; Yang, Q.; Zhang, X. F.; Hu, T. L.; Bu, X. H. *Dalton Trans.* **2010**, 56. (c) Zhu, A.-X.; Lin, J.-B.; Zhang, J.-P.; Chen, X.-M. *Inorg. Chem.* **2009**, *48*, 3882. (d) Lin, Y. Y.; Zhang, Y. B.; Zhang, J. P.; Chen, X. M. *Cryst. Growth Des.* **2008**, *10*, 3673.

(15) (a) Manson, J. L.; Lancaster, T.; Chapon, L. C.; Blundell, S. J.; Schlueter, J. A.; Brooks, M. L.; Pratt, F. L.; Nygren, C. L.; Qualls, J. S. *Inorg. Chem.* **2005**, *44*, 989. (b) Manson, J. L.; Lecher, J. G.; Gu, J.; Geiser, U.; Schlueter, J. A.; Hennig, R.; Wang, X.; Schultz, A. J.; Koo, H. J.; Whangbo, M. H. *Dalton Trans.* **2003**, 2905. (c) Dybisev, D. N.; Chun, H.; Yoon, S. H.; Kim, D.; Kim, K. *J. Am. Chem. Soc.* **2004**, *126*, 32.

(16) (a) Wang, X.-Y.; Wang, Z.-M.; Gao, S. *Chem Commun.* **2008**, 281. (b) Wang, Z. M.; Hu, K. L.; Gao, S.; Kobayashi, H. *Adv. Mater.* **2010**, *22*, 1526.

(17) (a) Wang, W. G.; Zhou, A. J.; Zhang, W. X.; Tong, M. L.; Chen, X. M.; Nakano, M.; Beedle, C. C.; Hendrickson, D. N. *J. Am. Chem. Soc.* **2007**, *129*, 1014. (b) Liu, T.; Zhang, Y. J.; Wang, Z. M.; Gao, S. *J. Am. Chem. Soc.* **2008**, *130*, 10500. (c) Zhang, Z. M.; Yao, S.; Li, Y. G.; Clérac, R.; Lu, Y.; Su, Z. M.; Wang, E. B. *J. Am. Chem. Soc.* **2009**, *131*, 14600. (d) Cadiou, C.; Coxall, R. A.; Graham, A.; Harrison, A.; Helliwell, M.; Parsons, S.; Winpenny, R. E. P. *Chem. Commun.* **2002**, 1106.

(18) Li, M. Y.; Ako, A. M.; Lan, Y. H.; Wernsdorfer, W.; Buth, G.; Anson, C. E.; Powell, A. K.; Wang, Z. M.; Gao, S. *Dalton Trans.* **2010**, 39, 3375.

(19) (a) Manoli, M.; Prescimone, A.; Bagai, R.; Mishra, A.; Murugesu, M.; Parsons, S.; Wernsdorfer, W.; Christou, G.; Brechin, E. K. *Inorg. Chem.* **2007**, *46*, 6968. (b) Ferguson, A.; Parkin, A.; Sanchez-Benitez, J.; Kamenev, K.; Wernsdorfer, W.; Murrie, M. *Chem. Commun.* **2007**, 3473. (c) Langley, S. J.; Helliwell, M.; Sessoli, R.; Rosa, P.; Wernsdorfer, W.; Winpenny, R. E. P. *Chem. Commun.* **2005**, 5029. (d) Andres, H.; Basler, R.; Blake, A. J.; Cadiou, C.; Chaboussant, G.; Grant, C. M.; Gudiel, H. U.; Murrie, M.; Parsons, S.; Paulsen, C.; Semadini, F.; Villar, V.; Wernsdorfer, W.; Winpenny, R. E. P. *Chem.—Eur. J.* **2002**, *8*, 4867.

(20) Schray, P. D.; Abbas, G.; Lan, Y.; Mereacre, V.; Sundt, A.; Dreiser, J.; Waldmann, O.; Kostakis, G. E.; Anson, C. E.; Powell, A. K. *Angew. Chem., Int. Ed.* **2010**, *49*, 5185.

$\text{Ln} = \text{Sm}$  (**1Sm**),  $\text{Gd}$  (**2Gd**),  $\text{Tb}$  (**3Tb**),  $\text{Dy}$  (**4Dy**),  $\text{Ho}$  (**5Ho**),  $\text{Er}$  (**6Er**), and  $\text{Y}$  (**7Y**) based on the reaction of  $\text{Mn}^{\text{II}}$  and  $\text{Ln}^{\text{III}}$  salts,  $\text{HCOOH}$ , propionic acid, and *N*-<sup>13</sup>Butyldiethanolamine (<sup>13</sup>Bu-deaH<sub>2</sub>) with triethylamine in MeOH. These compounds possess intriguing hetero-octanuclear ring structures with four  $\text{Mn}^{\text{III}}$  and four  $\text{Ln}^{\text{III}}$  ions alternatively arranged in a saddle-like manner representing the first  $\text{Mn}^{\text{III}}-\text{Ln}^{\text{III}}$  heterometallic rings. Furthermore, formate ion plays an important role in forming such a wheel structure.<sup>18</sup> The detailed syntheses, structures, and magnetic properties of this series will be carefully discussed.

## Experimental Section

**Reagents and General Procedures.** All reagents were obtained from commercial sources, and were used as received without further purification.  $\text{Mn}(\text{O}_2\text{CET})_2 \cdot 2\text{H}_2\text{O}$  was prepared according to literature.<sup>21</sup> All reactions were carried out under aerobic condition.

**Caution!** Perchlorate compounds are potentially explosive. They should be prepared in small quantities and handled with care.

**Synthesis of 1Sm–7Y.** At the first stage, the reaction of  $\text{Mn}(\text{O}_2\text{CET})_2 \cdot 2\text{H}_2\text{O}$ ,  $\text{Ln}(\text{NO}_3)_3 \cdot 6\text{H}_2\text{O}$ ,  $\text{HCOONa}$ , and <sup>13</sup>Bu-deaH<sub>2</sub> in 1:1:1:1 molar ratio in MeOH under stirring gave a red-brown solution from which fresh-red needle-like complexes of the series were obtained in one week with the yield of 20%–40%. Later on we found that these compounds can be obtained more conveniently by reaction of metal salts of  $\text{Mn}(\text{ClO}_4)_2 \cdot 6\text{H}_2\text{O}$  and  $\text{Ln}(\text{NO}_3)_3 \cdot 6\text{H}_2\text{O}$  with propionic acid, formic acid, and <sup>13</sup>Bu-deaH<sub>2</sub> with the addition of triethylamine. Typically, a solution of mixed <sup>13</sup>Bu-deaH<sub>2</sub> (1.0 mmol),  $\text{HCOOH}$  (3.0 mmol), propionic acid (1.0 mmol), and  $\text{NEt}_3$  (5.0 mmol) in MeOH (20 mL) was gently added into a solution of  $\text{Mn}(\text{ClO}_4)_2 \cdot 6\text{H}_2\text{O}$  and  $\text{Ln}(\text{NO}_3)_3 \cdot 6\text{H}_2\text{O}$  in MeOH (20 mL), and the mixture was sealed and left undisturbed. After one week X-ray quality crystals were obtained. Different reacting conditions like stirring, heating, and refluxing always led to the same product, and the use of mixed solvents of MeOH/ $\text{CH}_2\text{Cl}_2$  could improve the quality of crystals. **1Sm**, yield: 142 mg (45% based on Mn, the same below); anal. (%) calcd. for  $\text{C}_{68}\text{H}_{140}\text{Sm}_4\text{Mn}_4\text{N}_4\text{O}_{40}$ : C, 33.00; H, 5.70; N, 2.26; found: C, 32.50; H, 5.48; N, 2.24; selected IR data ( $\text{cm}^{-1}$ ): 576 (m), 772 (w), 812 (w), 892 (m), 1080 (s), 1294 (m), 1369 (s), 1412 (s), 1466 (s), 1587 (s), 2874 (m), 2962 (s), 3401 (b,s). **2Gd**, yield: 167 mg (53%); anal. (%) calcd. for  $\text{C}_{68}\text{H}_{140}\text{Gd}_4\text{Mn}_4\text{N}_4\text{O}_{40}$ : C, 32.64; H, 5.64; N, 2.24; found: C, 31.94; H, 5.49; N, 2.26; selected IR data ( $\text{cm}^{-1}$ ): 580 (m), 774 (m), 812 (w), 892 (m), 1009 (w), 1081 (s), 1291 (m), 1341 (s), 1367 (s), 1408 (s), 1466 (m), 1590 (s), 2874 (s), 2937 (s), 2960 (s), 3420 (b,s). **3Tb**, yield: 196 mg (60%); anal. (%) calcd. for  $\text{C}_{68}\text{H}_{140}\text{Tb}_4\text{Mn}_4\text{N}_4\text{O}_{40}$ : C, 32.55; H, 5.62; N, 2.23; found: C, 31.61; H, 5.46; N, 2.27; selected IR data ( $\text{cm}^{-1}$ ): 479 (w), 582 (m), 775 (m), 812 (w), 893 (m), 1010 (w), 1080 (s), 1166 (w), 1292 (m), 1340 (s), 1368 (s), 1408 (s), 1466 (s), 1591 (s), 2874 (s), 2938 (s), 2961 (s), 3399 (b,s). **4Dy**, yield: 135 mg (43%); anal. (%) calcd. for  $\text{C}_{68}\text{H}_{140}\text{Dy}_4\text{Mn}_4\text{N}_4\text{O}_{40}$ : C, 32.36; H, 5.59; N, 2.22; found: C, 31.75; H, 5.49; N, 2.21; selected IR data ( $\text{cm}^{-1}$ ): 479 (w), 581 (m), 776 (m), 812 (w), 892 (m), 1009 (w), 1081 (s), 1167 (w), 1291 (m), 1341 (s), 1367 (s), 1408 (s), 1466 (s), 1592 (s), 2874 (s), 2937 (s), 2960 (s), 3429 (b,s). **5Ho**, yield: 205 mg (66%); anal. (%) calcd. for  $\text{C}_{68}\text{H}_{140}\text{Ho}_4\text{Mn}_4\text{N}_4\text{O}_{40}$ : C, 32.24; H, 5.57; N, 2.21; found: C, 31.13; H, 5.57; N, 2.26; selected IR data ( $\text{cm}^{-1}$ ): 581 (m), 812 (w), 893 (m), 1009 (w), 1081 (s), 1296 (m), 1370 (s), 1418 (s), 1467 (s), 1589 (s), 2874 (s), 2937 (s), 2962 (s), 3419 (b,s). **6Er**, yield: 185 mg (57%); anal. (%) calcd. for  $\text{C}_{68}\text{H}_{140}\text{Er}_4\text{Mn}_4\text{N}_4\text{O}_{40}$ : C, 32.12; H, 5.55; N, 2.20; found: C, 31.62; H, 5.45; N, 2.30; selected IR data ( $\text{cm}^{-1}$ ): 598 (m), 777 (m), 812 (w), 893 (m), 1010 (w), 1082 (s), 1165 (w), 1292 (m), 1341 (m), 1369 (s), 1409 (s), 1467 (s), 1594 (s), 2874 (s), 2937 (s), 2961 (s), 3413 (b,s). **7Y**, yield: 72 mg (26%); anal. (%) calcd. for  $\text{C}_{68}\text{H}_{140}\text{Y}_4\text{Mn}_4\text{N}_4\text{O}_{40}$ : C, 36.64; H, 6.33; N, 2.51; found: C, 36.07; H, 6.22; N, 2.58; selected IR data ( $\text{cm}^{-1}$ ): 576 (m), 776 (w),

812 (w), 893 (m), 1010 (s), 1083(s), 1292 (m), 1369 (s), 1408 (s), 1467 (s), 1594 (s), 2874 (m), 2961 (s), 3421 (b,s).

**X-ray Crystallography.** The single crystal data at 150 K of compounds **1Sm**, **2Gd**, **5Ho**, **6Er**, and **7Y** were collected on the SCD beamline of the ANKA synchrotron at the Forschungszentrum Karlsruhe with a synchrotron radiation of wavelength  $\lambda = 0.80000 \text{ \AA}$ , using a Stoe IPDS II image plate diffractometer. For **3Tb** and **4Dy**, the data were collected at 100 K on a Bruker SMART Apex CCD diffractometer with  $\text{Mo K}\alpha$  radiation ( $\lambda = 0.71073 \text{ \AA}$ ) and were corrected semiempirically<sup>22,23</sup> for absorption. The structures were solved by direct methods, followed by full-matrix least-squares refinement against  $F^2$  using SHELXTL.<sup>22</sup> Anisotropic refinement was used for all non-H atoms; H atoms were placed in calculated positions. Powder X-ray diffraction (PXRD) patterns of all compounds were obtained on a Rigaku RINT2000 diffractometer at room temperature with  $\text{Cu K}\alpha$  radiation in a flat plate geometry.

**Physical Measurements.** Elemental analyses for C, H, and N were performed using an Elementar Vario MICRO CUBE analyzer. FTIR spectra were recorded using pure sample of the seven compounds in the range 4000–650  $\text{cm}^{-1}$  on a NICOLET iN10 MX spectrometer. Direct current (dc) and alternating current (ac) magnetic susceptibility measurements for the polycrystalline samples of the seven compounds were carried out on Quantum Design MPMS-XL7 and MPMS-XL5 SQUID magnetometers. Diamagnetic corrections were estimated using Pascal constants<sup>24</sup> and background correction by experimental measurement on sample holder. The magnetization study of **4Dy** at temperatures down to 40 mK was carried out on an array of micro-SQUIDS against a single crystal of **4Dy**.

## Results and Discussion

**Synthesis.** In this work, we selected one N-substituted diethanolamine, <sup>13</sup>Bu-deaH<sub>2</sub>, as the podal ligand. Similar ligands have been employed extensively to facilitate the formation of polynuclear species because their alcohol arms are good metal-bridging groups with versatile bridging modes.<sup>10b–f,25</sup> Although a variety of structure types with intriguing magnetic properties have been identified, they are mainly transition metal clusters.<sup>3,4,25</sup> Since Ln ions show strong affinity toward oxygen donors, we introduced them into the reaction system and indeed obtained the series 3d–4f mixed metal polynuclear species (see Experimental Section). When running through the whole  $\text{Ln}^{3+}$  series, we found that only the middle ones  $\text{Sm}^{3+}$ ,  $\text{Gd}^{3+}$ ,  $\text{Tb}^{3+}$ ,  $\text{Dy}^{3+}$ ,  $\text{Ho}^{3+}$  and adjacent heavy  $\text{Er}^{3+}$  and  $\text{Y}^{3+}$  can give the similar ring compounds. Reactions with lighter  $\text{Ln}^{3+}$  ions (like  $\text{La}^{3+}$ ,  $\text{Ce}^{3+}$ ,  $\text{Pr}^{3+}$ , and  $\text{Nd}^{3+}$ ) and heavier  $\text{Yb}^{3+}$  yielded no products. We assume that the light  $\text{Ln}^{3+}$  ions and  $\text{Yb}^{3+}$  might be either too big or too small for the formation of such rings (see later). It is worthy highlighting that the  $\text{HCOO}^-$  group is a key to the successful formation of such  $[\text{Mn}_4\text{Ln}_4]$  wheels. No crystalline products were obtained when  $\text{N}_3^-$  and  $\text{NO}_2^-$  were used in place of  $\text{HCOO}^-$  within the synthetic routes, and bulkier carboxylate ligands such as  $\text{OAc}^-$  and benzoate could not yield the same or even larger rings.

(22) Sheldrick, G. M. *SHELXTL*, version 6.14; Bruker AXS, Inc.: Madison, WI, 1997.

(23) Sheldrick, G. M. *SADABS (the Siemens Area Detector Absorption Correction)*; University of Göttingen: Göttingen, Germany, 1996.

(24) Mulay, L. N.; Boudreaux, E. A. *Theory and Applications of Molecular Diamagnetism*; John Wiley & Sons Inc.: New York, 1976.

(25) (a) Saalfrank, R. W.; Bernt, I.; Uller, E.; Hampel, F. *Angew. Chem., Int. Ed. Engl.* **1997**, *36*, 2482. (b) Watton, S. P.; Fuhrmann, P. L.; Pence, E.; Caneschi, A.; Comia, A.; Abbati, G. L.; Lippard, J. S. *Angew. Chem., Int. Ed. Engl.* **1997**, *36*, 2774. (c) Saalfrank, R. W.; Deutscher, C.; Spemer, S.; Nakajima, T.; Ako, A. M.; Uller, E.; Hampel, F.; Heinemann, F. W. *Inorg. Chem.* **2004**, *43*, 4372.

Table 1. Crystallographic Data and Structure Refinements for 1Sm-7Y

	1Sm	2Gd	3Tb	4Dy	5Ho	6Er	7Y
formula				C <sub>68</sub> H <sub>140</sub> Mn <sub>4</sub> Ln <sub>4</sub> N <sub>4</sub> O <sub>40</sub>			
formula weight	2475.00	2502.60	2509.28	2523.60	2533.32	2542.64	2229.24
crystal system	monoclinic	monoclinic	monoclinic	monoclinic	monoclinic	monoclinic	monoclinic
space group	C2/c	C2/c	C2/c	C2/c	C2/c	C2/c	C2/c
a, Å	40.1853(16)	40.1279(15)	40.0009(17)	39.9152(13)	40.015(4)	39.916(2)	39.996(4)
b, Å	8.7686(4)	8.7486(3)	8.6739(4)	8.6807(3)	8.7132(4)	8.7086(3)	8.6973(11)
c, Å	33.6509(14)	33.6560(12)	33.5212(14)	33.5003(11)	33.567(4)	33.396(2)	33.580(3)
β, deg	126.332(2)	126.379(2)	126.442(1)	126.373(1)	126.385(7)	126.377(4)	126.544(6)
V, Å <sup>3</sup>	9552.4(7)	9512.7(6)	9356.4(7)	9346.2(5)	9421.7(2)	9346.6(8)	9384.5(2)
Z	4	4	4	4	4	4	4
T, K	150	150	100	100	150	150	150
F(000)	4976	5008	5024	5040	5056	5072	4608
D <sub>C</sub> , g cm <sup>-3</sup>	1.781	1.747	1.781	1.793	1.786	1.807	1.578
μ, mm <sup>-1</sup>	4.122	4.582	3.588	3.763	3.920	5.766	3.049
λ, Å	0.80000	0.80000	0.71073	0.71073	0.80000	0.80000	0.80000
crystal size, mm <sup>3</sup>	0.17 × 0.04 × 0.02	0.13 × 0.02 × 0.01	0.16 × 0.11 × 0.06	0.28 × 0.06 × 0.03	0.13 × 0.06 × 0.03	0.15 × 0.08 × 0.02	0.23 × 0.04 × 0.02
T <sub>min</sub> and T <sub>max</sub>	0.330, 0.928	0.587, 0.956	0.598, 0.814	0.419, 0.896	0.493, 0.892	0.488, 0.878	0.541, 0.942
θ <sub>min</sub> , θ <sub>max</sub> , deg	1.69, 30.73	1.69, 29.93	2.66, 27.10	2.65, 26.73	2.82, 26.37	1.70, 30.60	1.51, 21.95
no. total reflns.	31082	27714	33340	21843	27069	27400	18080
no. uniq. reflns, R <sub>int</sub>	10232, 0.2350	9476, 0.1131	9893, 0.0258	9823, 0.0273	9468, 0.0967	9944, 0.1153	5716, 0.1163
no. obs. [I ≥ 2σ(I)]	7661	7945	9018	8175	6067	7569	3930
no. params	549	549	549	549	549	549	549
R1 [I ≥ 2σ(I)]	0.1052	0.0658	0.0265	0.0272	0.0734	0.0649	0.0749
wR2 (all data)	0.2888	0.2059	0.0671	0.0624	0.1885	0.1795	0.2038
S	1.027	1.115	1.043	1.035	0.999	1.020	1.020
Δρ <sup>a</sup> , e/Å <sup>3</sup>	+3.42, -3.22	+4.29, -2.28	+1.06, -0.78	+1.17, -0.70	+1.02, -2.79	+2.72, -2.26	+0.48, -1.78
max. and mean Δ/σ <sup>b</sup>	0.002, 0.000	0.000, 0.000	0.002, 0.000	0.002, 0.000	0.001, 0.000	0.001, 0.000	0.009, 0.000

<sup>a</sup> Max and min residual density. <sup>b</sup> Max and mean shift/σ.

**Crystal Structures.** The seven compounds are iso-structural, and this is identified by their very similar IR spectra (Supporting Information, Figure S1) and PXRD patterns (Supporting Information, Figure S2), as well as the single crystal structure analysis (Table 1). All the compounds crystallize in the monoclinic space group C2/c. The structure consists of neutral octa-nuclear molecules (Figure 1a and 1b) possessing an eight-member [Mn<sub>4</sub>Ln<sub>4</sub>] saddle-like ring core, with four Mn<sup>III</sup> and four Ln<sup>III</sup> ions alternatively arranged. Part of the ring is similar to the heterometallic semicircular [Mn<sup>III</sup><sub>2</sub>Ln<sup>III</sup><sub>3</sub>] strands recently reported.<sup>26</sup> The four Mn ions are nearly coplanar, and two Ln ions above and the other two below the Mn<sub>4</sub> plane (Figure 1b). The [Mn<sub>4</sub>Ln<sub>4</sub>] ring locates on a crystallographic 2-fold axis through the center and perpendicular to the Mn<sub>4</sub> plane. Each Mn<sup>III</sup> ion is six-coordinate and exhibits an elongated octahedral environment completed by two alkoxide arms and N atom of one <sup>n</sup>Bu-dea, and three O atoms from one bridging MeO<sup>-</sup>, one *syn-syn/anti* HCOO<sup>-</sup> and one *syn-syn* EtCOO<sup>-</sup>, with the axial positions occupied by the N atom of <sup>n</sup>Bu-dea and one *syn*-O end of HCOO<sup>-</sup>. The Mn–O/N distances are 1.901(2)–1.979(8) Å for the equatorial O atoms and 2.167(7)–2.351(7) Å for the axial O/N ones (Table 2). These bond distances around Mn<sup>III</sup> ions are in the expected range of those found in octahedrally coordinated Mn<sup>III</sup> complexes with N/O ligation.<sup>10b–f,26</sup> The observed Jahn–Teller elongation for Mn ions confirms that they are trivalent<sup>27</sup> though the divalent Mn salts were used in synthesis. The *cis* O–Mn–O/N angles range between 78.9(3)–104.1(3)° and *trans* ones 157.2(3)–177.0(3)°.

The four Jahn–Teller axes of Mn<sup>III</sup> (yellow bonds in Figure 1a and 1b) are alternately tilted with respect to each other. Each Ln<sup>III</sup> ion is eight-coordinated in a bicapped trigonal prism geometry comprising an O<sub>8</sub> donor set derived from two *syn-syn/anti* HCOO<sup>-</sup>, one terminal MeOH, one bridging MeO<sup>-</sup>, one monocoordinating and one *syn-syn* bridging EtCOO<sup>-</sup> ligands, and two alkoxide arms from two neighboring <sup>n</sup>Bu-dea ligands. The requirement of coordination number (CN) of 8 for the Ln ions within this kind of structure is probably the origin for the experimental observation that such structure could not be obtained for the lighter and heavier Ln<sup>3+</sup> because the larger lighter Ln<sup>3+</sup> ions prefer CN = 9 while the smaller heavier Ln ions like CN = 7.<sup>28</sup> The Ln–O distances are in the range 2.273(7)–2.490(8) Å and O–Ln–O angles 62.8(3)–157.9(3)° (Table 2). The four *syn-syn/anti* HCOO<sup>-</sup> inside the ring each connects one Mn<sup>III</sup> (*syn*-end of *syn/anti*) and its two neighboring Ln<sup>III</sup> (*syn-anti*). Each alkoxide arm of the four <sup>n</sup>Bu-dea bridges one pair of Mn–Ln. The Mn–Ln pairs not bridged by *syn-syn* HCOO<sup>-</sup> linkage are connected by a *syn-syn* EtCOO<sup>-</sup>, while those with the *syn-syn* HCOO<sup>-</sup> bridges have an extra μ-OMe linkage. Therefore, in the ring each Mn–Ln pair has two μ-O atoms and one *syn-syn* carboxylate to link the metal ions though the linkages come from different ligands. The Mn···Ln distances range from 3.351(4) to 3.575(3) Å (Table 2), comparable with that in the semicircular [Mn<sup>III</sup><sub>2</sub>Ln<sup>III</sup><sub>3</sub>] strands.<sup>26</sup> Inside the ring, the *syn-anti* formate bridged Ln···Ln separation is 5.9150(6) to 6.0373(8) Å, and the Mn···Mn distances

(26) Akhtar, M. N.; Zheng, Y. Z.; Lan, Y. H.; Mereacre, V.; Anson, C. E.; Powell, A. K. *Inorg. Chem.* **2009**, *48*, 3502.

(27) Casey, A. T.; Mitra, S. In *Theory and Application of Molecular Paramagnetism*; Mulay, L. N., Boudreaux, E. A., Eds.; John Wiley & Sons Inc.: New York, 1976; pp 179, 271–316.

(28) (a) He, Z.; Gao, E. Q.; Wang, Z. M.; Yan, C. H.; Kurmoo, M. *Inorg. Chem.* **2005**, *44*, 862. (b) Deng, Z. P.; Kang, W.; Huo, L. H.; Zhao, H.; Gao, S. *Dalton Trans.* **2010**, 39, 6276. (c) Wang, H. Y.; Cheng, J. Y.; Ma, J. P.; Dong, Y. B.; Huang, R. Q. *Inorg. Chem.* **2010**, *49*, 2416. (d) Xiang, S. C.; Hu, S. M.; Sheng, T. L.; Chen, J. S.; Wu, X. T. *Chem.—Eur. J.* **2009**, *15*, 12496. (e) Zhao, X. Q.; Zhao, B.; Wei, S.; Cheng, P. *Inorg. Chem.* **2009**, *48*, 11048.

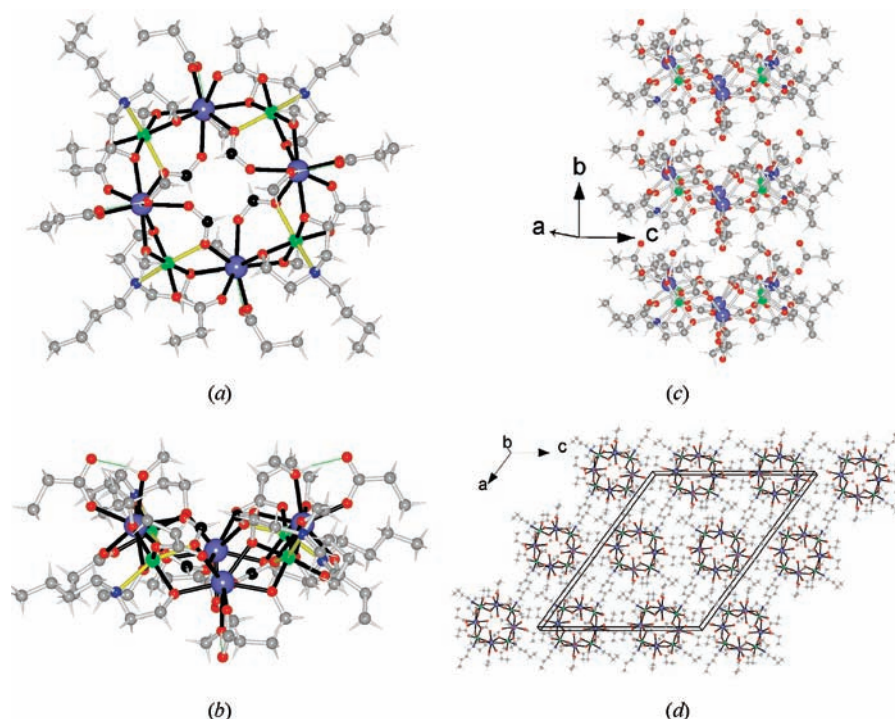


**Figure 1.** Structure of the iso-structural series, drawn based on the structure data of **4Dy**, (a) top view and (b) side view of the octa-nuclear  $\text{Mn}_4\text{Ln}_4$  molecule; (c) the molecular column consisting of three individual molecules; and (d) the nearly hexagonal closest packing of the columns (one molecular layer only) viewed along  $b$  direction in the lattice. In (a) and (b) the Jahn–Teller axes of  $\text{Mn}^{\text{III}}$  are shown in yellow bonds, and the bonds around metal ions are highlighted in black, and thin green bonds are the intramolecular H-bonds (see text). In (d) the bonds around metal ions are also highlighted in black. Atomic color scheme: Mn, green; Ln, blue violet; O, red; N, blue; C of formate, black in (a) and (b); other C, gray; H, white.

**Table 2.** Selected Bond Distances (Å) and Angles (deg) in **1Sm–7Y**

	<b>1Sm</b>	<b>2Gd</b>	<b>3Tb</b>	<b>4Dy</b>	<b>5Ho</b>	<b>6Er</b>	<b>7Y</b>
Ln–O	2.357(9)–2.490(8)	2.330(6)–2.466(5)	2.313(2)–2.456(2)	2.301(2)–2.441(2)	2.303(9)–2.433(8)	2.273(7)–2.424(5)	2.294(8)–2.427(7)
Mn–O <sub>equatorial</sub>	1.915(9)–1.979(8)	1.912(6)–1.968(6)	1.898(2)–1.960(2)	1.898(2)–1.958(2)	1.902(9)–1.958(8)	1.904(7)–1.966(6)	1.897(7)–1.948(7)
Mn–O/N <sub>axial</sub>	2.185(7)–2.343(1)	2.186(5)–2.351(7)	2.179(2)–2.338(3)	2.173(2)–2.343(3)	2.180(8)–2.335(1)	2.170(5)–2.340(7)	2.178(7)–2.343(9)
Mn–Ln	3.412(3)–3.575(3)	3.394(1)–3.561(1)	3.374(5)–3.542(5)	3.361(6)–3.534(5)	3.356(2)–3.530(2)	3.351(4)–3.521(1)	3.352(2)–3.530(2)
<i>cis</i> O/N–Mn–O/N	79.2(3)–103.2(4)	79.2(2)–103.8(3)	79.4(9)–102.7(1)	79.4(1)–102.9(1)	79.5(3)–103.5(3)	79.0(2)–104.1(3)	78.9(3)–103.0(3)
<i>trans</i> O–Mn–O/N	157.9(3)–177.0(3)	157.6(3)–176.0(2)	158.2(1)–176.3(1)	157.8(1)–176.1(1)	157.7(4)–175.1(3)	157.2(3)–175.7(3)	157.7(3)–176.4(3)
O–Ln–O	62.8(3)–157.9(3)	63.3(2)–157.1(2)	63.7(1)–156.9(1)	63.82(8)–156.9(8)	64.0(3)–156.8(3)	64.0(3)–156.1(2)	63.9(2)–156.6(2)
Mn–O–Ln	99.1(3)–110.8(4)	99.4(2)–110.1(2)	99.2(1)–110.4(1)	99.4(1)–110.6(1)	99.6(3)–110.6(4)	99.6(2)–110.7(0)	99.6(3)–111.0(3)

separated by one Ln are 6.398(2) to 6.507(2) Å. The Mn–O–Ln angles vary between 99.1(3) to 111.0(3)°. There is a hydrogen bond formed between the terminal MeOH and the monocoordinating EtCOO<sup>−</sup> on the same Ln<sup>III</sup> ion with O–H···O distance of 2.56(2)–2.60(2) Å. In the lattice, the molecules stack into columns along the  $b$  direction, and the columns further arrange in a nearly hexagonal closest packing extending along  $a$  and  $c$  directions (Figure 1c and 1d). Between the molecules there are only weak van der Waals interactions, and the molecular bulky organic shells separate the magnetic cores of individual molecules well in lattice. When running through the series, the cell parameters and atomic distances (Table 1 and 2) show the decrease tendency in accord with the lanthanide contraction, as observed in other iso-structural Ln compounds.<sup>28,10d,10e</sup>

**Magnetic Properties.** The temperature dependence of the dc magnetic susceptibility ( $\chi$ , per  $\text{Mn}_4\text{Ln}_4$ ) data for the seven compounds were collected in the range of 1.8 to 300 K

under 1 kOe field (Figure 2a), and the basic magnetic data derived from these measurements are listed in Table 3. The room temperature  $\chi T$  values for the seven compounds are in good agreement with the expected values<sup>27,29</sup> for isolated four Mn<sup>III</sup> and four Ln<sup>III</sup>. On lowering temperature from 300 to 50 K, all compounds have their  $\chi T$  values decreasing slowly, and that of **2Gd** and **7Y** almost keep constant. In lower temperature region, the  $\chi T$  values decrease more quickly except that of **3Tb**. The susceptibility data in the high temperature region (above 15 K) could be fitted to the Curie–Weiss law and the derived Curie constants ( $C$ ) and Weiss temperatures ( $\theta$ ) are summarized in Table 3. All compounds have small negative  $\theta$  values. However, it is difficult to evaluate if these small Weiss temperatures and the decrease of  $\chi T$  on cooling indicate antiferromagnetic interactions within the materials because of the presence of strong spin–orbital coupling effects in both Ln<sup>III</sup> and Mn<sup>III</sup> ions, as in many other Ln<sup>III</sup>–Mn<sup>III</sup> systems.<sup>9d–g,10</sup> **2Gd** and **7Y** with isotropic Gd<sup>III</sup> and non-magnetic Y<sup>III</sup> have very small negative Weiss temperatures which could also be due to the anisotropic Mn<sup>III</sup> ions.<sup>10d,e</sup> For **3Tb** the  $\chi T$  product decreases to a minimum of 50.4 cm<sup>3</sup> K mol<sup>−1</sup> around 13 K then

(29) (a) Benelli, C.; Gatteschi, D. *Chem. Rev.* **2002**, *102*, 2369. (b) Kahn, M. L.; Sutter, J.-P.; Golhen, S.; Guionneau, P.; Ouahab, L.; Kahn, O.; Chasseau, D. *J. Am. Chem. Soc.* **2000**, *122*, 3413. (c) Kahn, O. *Molecular Magnetism*; VCH: Weinheim, 1993.

Table 3. Summary of Static Magnetic Properties of 1Sm-7Y

	1Sm	2Gd	3Tb	4Dy	5Ho	6Er	7Y
ground state of Ln	$^6H_{5/2}$	$^8S_{7/2}$	$^7F_6$	$^6H_{15/2}$	$^5I_8$	$^4I_{15/2}$	
expected $\chi T$ at 300 K, $\text{cm}^3 \text{K mol}^{-1}$	12.36	43.52	59.28	68.68	68.28	57.92	12.00
observed $\chi T$ at 300 K, $\text{cm}^3 \text{K mol}^{-1}$	10.99	43.08	57.82	69.32	68.70	57.07	11.14
observed $\chi T$ at 1.8 K, $\text{cm}^3 \text{K mol}^{-1}$	6.25	14.09	58.32	15.60	26.08	21.60	8.14
<sup>a</sup> Curie constant $C$ , $\text{cm}^3 \text{K mol}^{-1}$	11.44	43.52	58.72	70.77	70.87	58.55	11.10
<sup>a</sup> Weiss constant $\theta$ , K	-12.8	-2.6	-4.3	-5.9	-10.1	-6.6	-1.3
magnetization at 70 kOe, 2K, $N\beta$	8.72	38.90	30.83	33.70	32.59	34.42	11.75
<sup>b</sup> saturation magnetization, $N\beta$	18.86	44.00	52.00	56.00	56.00	52.00	16.00

<sup>a</sup>Curie–Weiss fitting were performed upon susceptibility data in the temperature range 15–300 K for all compounds. <sup>b</sup>Assume  $M_S$  = sum of  $g_J$  ( $\text{Ln}^{3+}$ ) and  $g_S$  ( $\text{Mn}^{3+}$ ,  $g = 2$ ,  $S = 2$ )

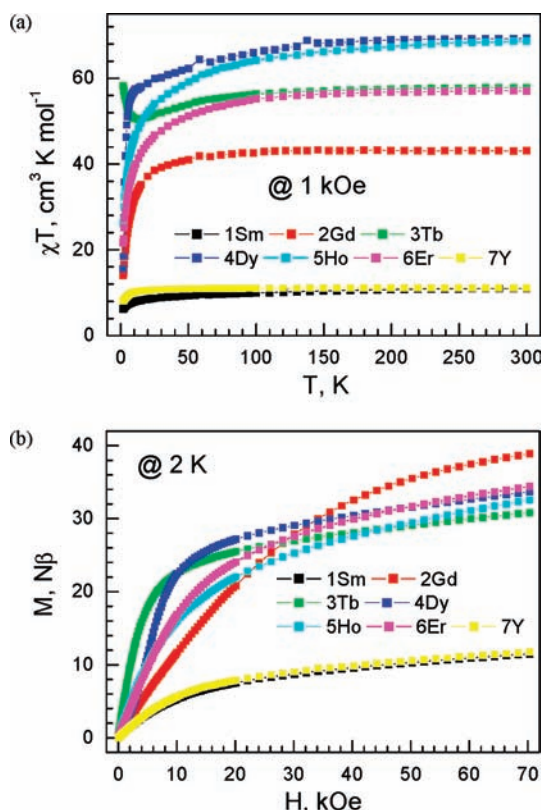


Figure 2. Static magnetic properties of the seven compounds, (a) plots of  $\chi T$  versus  $T$  under 1 kOe, (b) the isothermal magnetization plots at 2 K.

increases up to  $58.32 \text{ cm}^3 \text{K mol}^{-1}$  at 1.8 K. The low temperature increase of the  $\chi T$  product may be due to the possible ferrimagnetic arrangement of the spins in **3Tb**.<sup>26</sup> The isothermal magnetization data ( $M$  vs  $H/T$ , Supporting Information, Figure S3) for the seven compounds at 2, 3, and 5 K are not superposed on a master-curve as expected for isotropic systems with a well-defined ground state, suggesting the presence of a significant magnetic anisotropy and/or low-lying excited states as expected for compounds containing anisotropic  $\text{Mn}^{\text{III}}$  and  $\text{Ln}^{\text{III}}$  ions, even for **2Gd** and **7Y** with isotropic  $\text{Gd}^{\text{III}}$  and non-magnetic  $\text{Y}^{\text{III}}$ . The  $M$  versus  $H$  curves at 2 K do not show any sign of significant hysteresis effect, and the magnetization increases smoothly at low fields, followed by an almost linear increase without clear saturation up to 7 T (Figure 2b), where it reaches 11.5 (**1Sm**), 38.9 (**2Gd**), 30.8 (**3Tb**), 33.7 (**4Dy**), 32.6 (**5Ho**), 34.4 (**6Er**), and 11.8 (**7Y**)  $N\beta$ . These results prove again the presence of a significant magnetic anisotropy in these systems as expected using  $\text{Mn}^{\text{III}}$  and anisotropic  $\text{Ln}^{\text{III}}$  ions.

The ac susceptibility measurements on these compounds in zero dc field were performed to probe the presence of magnetization slow relaxation (i.e., SMM properties). **2Gd**,<sup>18</sup> **5Ho**, and **6Er** show negligible out-of-phase ( $\chi''$ ) components (data not involved) confirming that the three compounds do not behave as SMMs above 1.8 K; thus, no further study applied. **1Sm**, **3Tb**, and **4Dy**<sup>18</sup> exhibit clear frequency dependent  $\chi''$  signals, suggesting that they behave as SMMs (Supporting Information, Figure S4). For **7Y**, the ac susceptibility measurements show the appearance of a very weak and noisy  $\chi''$  signal at 1 kHz, and its dynamic magnetization was further investigated by applying a dc magnetic field.

As shown in the Supporting Information, Figure S4c, the peaks of  $\chi''$  signals for **4Dy** could only be detected for frequencies higher than 1100 Hz above 1.8 K,<sup>18</sup> the low temperature limit of our squid instruments. The ac data between 1100 and 1500 Hz of **4Dy** are used to determine the relaxation time ( $\tau$ ) and its temperature dependence, which roughly follows a thermally activated behavior (Arrhenius law:  $\tau = \tau_0 \exp(E_a/k_B T)$ ) with an energy gap ( $E_a/k_B$ ) of 12 K and a pre-exponential factor  $\tau_0 = 3.5 \times 10^{-7} \text{ s}$ ,<sup>18</sup> which is comparable to those estimated for similar 3d-4f SMM systems.<sup>8,10</sup> The magnetization of **4Dy** was further studied on field-oriented single crystals by micro-SQUID<sup>30</sup> at temperatures down to 40 mK (Figure 3). Hysteresis loops were observed with characteristics of SMMs. The coercivities increase with decreasing temperature and with increasing sweeping rate, as expected for the superparamagnet-like behavior of a SMM. The dominating feature in these loops is a one-step behavior that is typical for SMMs with very slow zero-field relaxation.<sup>31</sup>

Although the relaxation observed by the ac technique for **1Sm** and **3Tb** is clearly frequency-dependent (Supporting Information, Figures S4a, S4b), the relaxation time of the magnetization cannot be deduced because the relaxation mode is at higher frequencies than the highest experimentally available frequency of 1500 Hz for our instruments. Such behavior can be due to temperature-independent zero-field fast quantum tunneling of the magnetization (QTM), and the application of a small external field can remove the degeneracy of the  $m_S$  states and lower the probability of the zero-field QTM between the  $\pm m_S$  states.<sup>32</sup> For **1Sm**, the frequency dependence

(30) (a) Wernsdorfer, W. *Adv. Chem. Phys.* **2001**, *118*, 99. (b) Wernsdorfer, W. *Supercond. Sci. Technol.* **2009**, *22*, 064013.

(31) (a) Tang, J.; Hewitt, I.; Madhu, N. T.; Chastanet, G.; Wernsdorfer, W.; Anson, C. E.; Benelli, C.; Sessoli, R.; Powell, A. K. *Angew. Chem., Int. Ed.* **2006**, *45*, 1729. (b) Aronica, C.; Pilet, G.; Chastanet, G.; Wernsdorfer, W.; Jacquot, J. F.; Luneau, D. *Angew. Chem., Int. Ed.* **2006**, *45*, 4659.

(32) Gatteschi, D.; Sessoli, R.; Villain, J. *Molecular Nanomagnets*; Oxford University Press: Oxford, 2006.

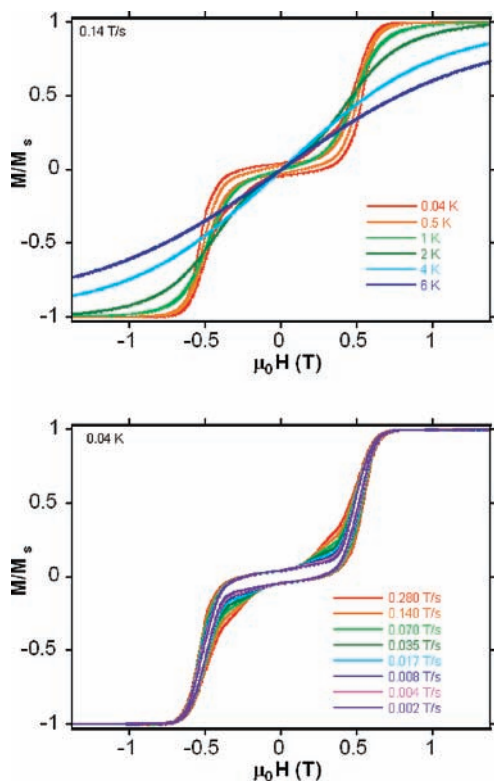


**Figure 3.** Hysteresis loops of the normalized magnetization at the indicated temperatures and field sweeping rate 0.14 T/s (top) and at the indicated field sweeping rates and 0.04 K (bottom) for a single crystal of **4Dy** oriented along the easy direction of magnetization.

of the ac susceptibility data at 1.8 K has been studied by applying a small dc field up to 3500 Oe (Supporting Information, Figure S5). As expected, the zero-field QTM is partially suppressed. The peak of  $\chi''$  signal moves to low frequencies and above 2 kOe the peak does not shift. Therefore, a field of 2000 Oe is selected to investigate the frequency and temperature dependence of the ac susceptibility of **1Sm** (Figure 4). To better characterize the time distribution for relaxation,  $\chi''$  versus  $\chi'$  (in-phase signal) data (Figure 5) under different temperatures and dc field, fields were fitted by the extended Debye Model using eq 1,<sup>33</sup> in which  $\chi_T$  is the isothermal susceptibility,  $\chi_S$  the adiabatic susceptibility,  $\omega$  the angular frequency of the ac field, and  $\tau$  the relaxation time of the system at the temperature at which the fit is performed. The parameter  $\alpha$  takes into account the width of the distribution, being zero for a single relaxation process.

$$\chi(\omega) = \chi_s + \frac{\chi_T - \chi_S}{1 + (i\omega\tau)^{1-\alpha}} \quad (1)$$

All derived parameters were summarized in the Supporting Information, Tables S1 and S2; the small  $\alpha$  values less than 0.13 are compatible with the SMM behavior. The temperature dependence of the relaxation time can be described by the Arrhenius law, with  $\tau_0 = 4.9 \times 10^{-8}$  s, and the energy barrier of 15 K (Supporting Information, Figure S6). Thus, the relaxation process of **1Sm** is expected to be dominated by the two-phonon (Orbach) process in the observed temperature range.<sup>34</sup>

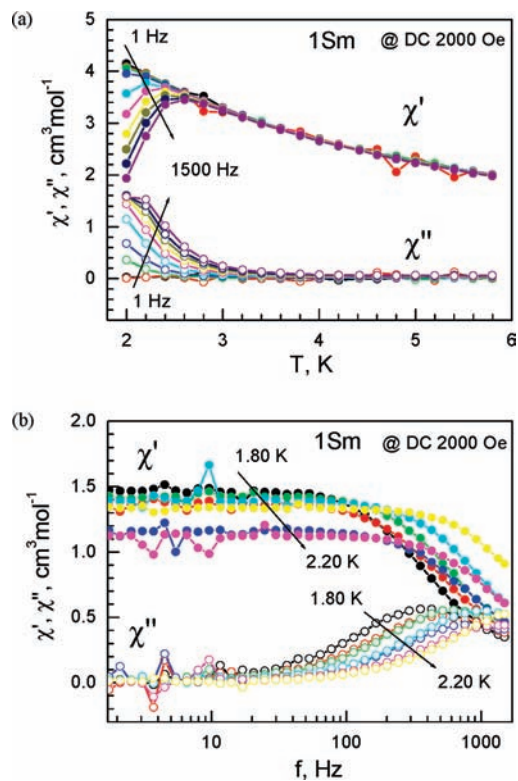


**Figure 4.** (a) Temperature dependence of ac susceptibilities under a dc field of 2 kOe for **1Sm** with an oscillating field of 3 Oe at different frequencies. (b) The frequency dependence of ac susceptibilities under a dc field of 2 kOe for **1Sm** with an oscillating field of 3 Oe between 1.80 K–2.20 K.

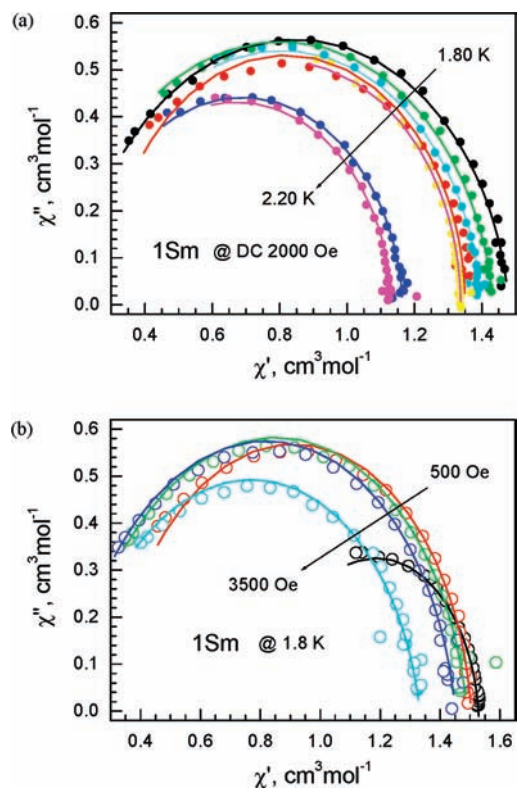


**Figure 5.** Cole–Cole diagram taken for **1Sm** under different temperatures (filled symbols) (a) and different dc fields (open symbols) (b). The lines represent the best-fit calculated values with an extended Debye model.

(33) Cole, K. S.; Cole, R. H. *J. Chem. Phys.* **1941**, *9*, 341.

(34) (a) Pointillart, F.; Bernot, K.; Sessoli, R.; Gatteschi, D. *Chem.—Eur. J.* **2007**, *13*, 1602. (b) Orbach, R. *Proc. Roy. Soc. A* **1961**, *264*, 485.

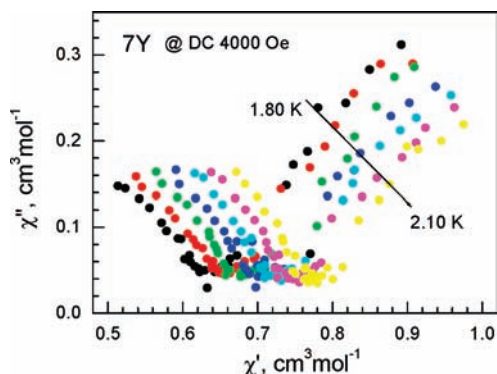


**Figure 6.** Cole–Cole diagram taken for **7Y** in the temperature range 1.80–2.10 K under a dc field of 4000 Oe.

This process is thermally activated and leads to the exponential temperature dependence of the relaxation time. SMM behavior has been observed very recently for a  $\text{Fe}_{12}\text{Sm}_4$  cluster compound composed of  $\text{Fe}^{\text{III}}$  and  $\text{Sm}^{\text{III}}$  ions.<sup>35</sup> For **3Tb**, the ac susceptibility under 10 Hz was measured by scanning dc fields from 0 to 10 kOe, no proper dc field was found to suppress the zero-field quantum tunneling efficiently.

The dynamics of the magnetization of **7Y** was studied by the same methods. Frequency-dependent  $\chi''$  signals were observed under a dc field of 4000 Oe (Supporting Information, Figure S7). Noteworthy is that **7Y** exhibits two relaxation processes as evidenced by the Cole–Cole plots in Figure 6. Although the high frequency and low frequency peaks of  $\chi''$  signals were not observed between 1–1000 Hz, the Cole–Cole plots in the temperature range of 1.80–2.10 K clearly display two distinguished relaxation phases.<sup>36</sup> Besides, the Cole–Cole diagram under different dc fields also reveals a multiple relaxation process (Supporting Information, Figure S8). The two relaxation processes should originate only from the  $\text{Mn}^{\text{III}}$  ions, since  $\text{Y}^{\text{III}}$  is diamagnetic. We tried to fit the data by extended Debye models, but failed because of the poor quality of the experimental data.

In our investigation, the SMM behavior observed in compounds **1Sm**, **3Tb**, **4Dy**, and **7Y** is attributed to the magnetic anisotropy of both  $\text{Mn}^{\text{III}}$  and  $\text{Ln}^{\text{III}}$  ( $\text{Ln} = \text{Tb}$  and

$\text{Dy}$ ) ions as in other 3d-4f cases. However, the introduction of the high anisotropic  $\text{Tb}^{\text{III}}/\text{Dy}^{\text{III}}$  ions did not increase efficiently the energy barrier of the SMMs as compared to that of **1Sm**. In the structure, four  $\text{Mn}^{\text{III}}$  and four  $\text{Ln}^{\text{III}}$  ions alternatively arranged in a saddle-like ring with four  $\text{Mn}^{\text{III}}$  ions nearly coplanar, and two  $\text{Ln}^{\text{III}}$  ions above and the other two below the  $\text{Mn}_4$  plane. The Jahn–Teller axes of  $\text{Mn}^{\text{III}}$  ions (as represented in yellow bonds in Figure 1a) are tilted with respect to each other, and leads to a strong reduction of the magnetic anisotropy of  $\text{Mn}^{\text{III}}$  ions. In spite of this, the easy axes of magnetization of  $\text{Ln}^{\text{III}}$  ions are non-collinear, which also decreases the anisotropy of the whole molecule. In our case, the series of compounds display a typical geometrical reduction of the Ising anisotropy, proving that the molecular geometry and local symmetry of the anisotropic ions are the key factors in designing SMMs with higher energy barrier.

## Conclusion

We have reported here the syntheses and the structural and magnetic properties of seven isostructural  $[\text{Mn}_4\text{Ln}_4]$  ring compounds. They are the first series of Mn–Ln saddle-like wheel complexes incorporating formate as key carboxylate bridges. The synthetic methodology of employing formate ion, the smallest carboxylate, in the present work provides a useful approach for assembling 3d-4f metal clusters through variation of the 3d and 4f sources. The investigation of dynamics of the magnetization for **1Sm**, **3Tb**, **4Dy**, and **7Y** reveals that they exhibit SMM behavior, while **7Y** displays a multiple relaxation process. Single crystal magnetic measurement confirms **4Dy** as a new SMM. These results have shown that the dynamics of the magnetization and the relaxation behavior of the compounds were dominated by both  $\text{Mn}^{\text{III}}$  and  $\text{Ln}^{\text{III}}$  ions and that the substitution of lanthanide ions in mixed  $\text{Ln}^{\text{III}}\text{-Mn}^{\text{III}}$  complexes affects the nature of the low-temperature magnetic behavior. Further experiments are underway to quantify the different contributions to this behavior, such as studies on analogues with diamagnetic  $\text{Co}^{\text{III}}$  ions.

**Acknowledgment.** This work was supported by the NSFC (Grants 20871007, 20821091), and the National Basic Research Program of China (Grant 2006CB601102, 2009CB929403).

**Supporting Information Available:** Table S1 and S2, Figure S1 to S8, and CIF files of crystallography data for the structures in this work. This material is available free of charge via the Internet at <http://pubs.acs.org>.

(35) Zeng, Y.-F.; Xu, G.-C.; Hu, X.; Chen, Z.; Bu, X.-H.; Gao, S.; Sañudo, E. C. *Inorg. Chem.* **2010**, ASAP, DOI: 10.1021/ic1009708.

(36) Guo, Y. N.; Xu, G. F.; Gamez, P.; Zhao, L.; Lin, S. Y.; Deng, R. P.; Tang, J. K.; Zhang, H. J. *J. Am. Chem. Soc.* **2010**, *132*, 8538.